

Magneto-Optic Characterization of Defects and Study of Flux Avalanches in High- T_c Superconductors down to Nanosecond Time Resolution

B.-U. Runge, U. Bolz, J. Boneberg, V. Bujok, P. Brüll, J. Eisenmenger, J. Schiessling, and P. Leiderer

University of Konstanz, Faculty of Physics, D-78457, Konstanz, Germany

e-mail: bernd-uwe.runge@uni-konstanz.de

Received September 9, 1999

Abstract—Optical methods offer an intrinsic high potential for experiments with excellent spatial and in particular also temporal resolution. Using the Faraday effect we carried out magneto-optical investigations of high- T_c superconductor thin films in a polarization microscope. Small defects in the superconducting material which possess a lower critical current density disturb the homogeneous penetration of magnetic flux into a sample when an external magnetic field is applied after zero field cooling. This is true even if the defects are below the sample surface or when the superconducting sample is covered by a thin layer of another material, e.g., gold, and can be used to characterize samples with diameters up to 3". For studies of the dynamics of magnetic flux in a superconducting sample, a pump-probe setup has been used. An instability which causes magnetic flux to enter the sample in dendritic form [1] is triggered by local heating with a focused ns or fs laser pulse. Part of the beam is separated by a beam splitter, passed through a variable delay line of suitable length and used for illumination of the sample. For $\text{YBa}_2\text{Cu}_3\text{O}_{7-\delta}$ thin films a spreading velocity of $(5 \pm 2) \times 10^4$ m/s is found which is an order of magnitude higher than the velocity of sound. The total area of the dendritic structure formed is found to depend linearly on the change ΔB_{ext} of the external magnetic flux density applied before the trigger pulse. No dependence on the pulse duration has been observed, suggesting a purely thermal nature of the trigger process.

1. INTRODUCTION

The penetration of magnetic flux into superconductors is of fundamental importance for the understanding of superconductivity as well as for its applications. Therefore in the past this has been the topic of numerous investigations carried out either with conventional type II superconductors [2, 3] or with high- T_c materials [4–6]. These studies have confirmed theories of the critical state in thin type II superconducting layers [7–9]. In this context, optical methods have proven very useful as they offer an intrinsic high potential for experiments with excellent spatial, and, in particular, also temporal resolution.

2. EXPERIMENTAL SETUP

In principle magneto-optic experiments can be carried out using either the Faraday or the magneto-optical Kerr effect, both giving rise to a rotation of the plane of polarization of linearly polarized light proportional to the local magnetic field at the sample. One can then visualize the flux distribution as optical contrasts in a polarization microscope. As high- T_c superconductors (HTSC) like $\text{YBa}_2\text{Cu}_3\text{O}_{7-\delta}$ (YBCO) show only

extremely small Kerr rotations, all experiments presented in this paper are based on the Faraday effect, i.e., the rotation of the polarization plane of light which passes a magneto-optically active layer exposed to the magnetic field of the underlying superconductor. The magneto-optical layer can either consist of EuS [10] or of an in-plane magnetized iron garnet film [11, 12] deposited on a separate substrate and spring loaded against the sample as sketched in Fig. 1. In both cases the use of a separate substrate offers high flexibility in the experiment as the sample can easily be changed without the need for a new indicator film and, more importantly, without permanent modification of the sample which might prevent it from being used for different purposes. While using the EuS layer limits the operating temperature range to ≤ 20 K, suitable iron garnet films operate almost as well even up to room temperature. In order to achieve high time resolution, a pump-probe technique can be used where part of the beam of a pulse laser is used to trigger an event whereas a second part is fed through an optical delay line of e.g., several 10 ns and then used to illuminate the sample, hence probing its state at a well defined time shortly after the trigger pulse. Figure 4 shows a schematic drawing of the pump-probe setup.

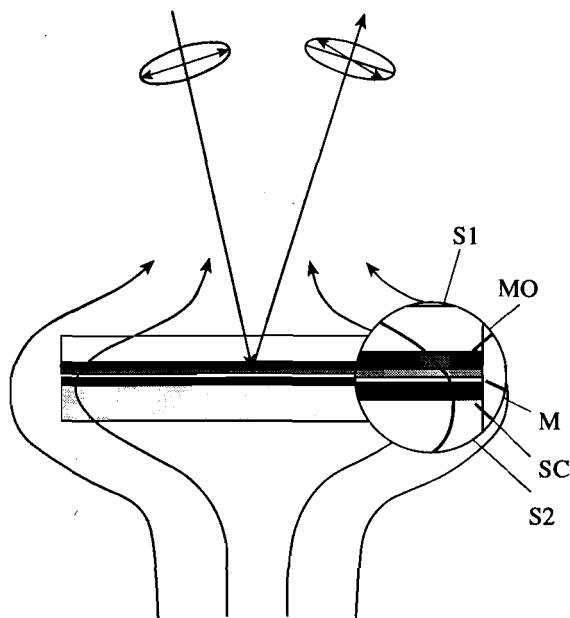


Fig. 1. Schematic drawing of the sample. The incoming light is linearly polarized. S1 = substrate for MO, S2 = substrate for SC, MO = magneto-optically active layer, SC = superconducting sample, M = aluminum mirror.

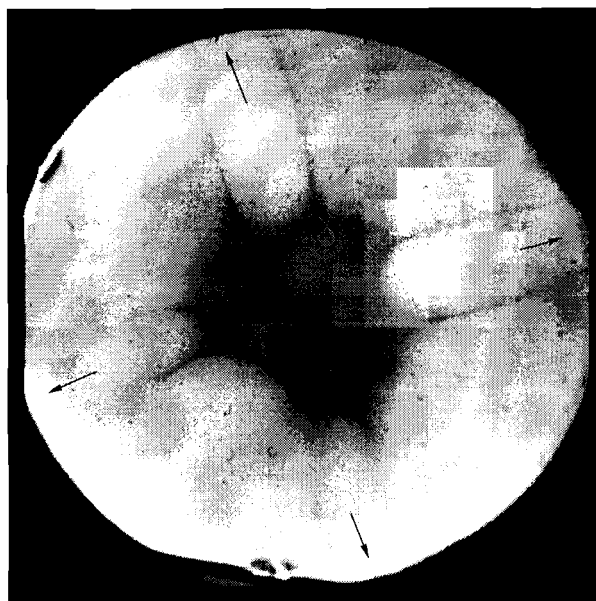


Fig. 2. Flux distribution of a 3" double-sided YBCO-Wafer at 10 K (ZFC) at a homogeneous magnetic field of 86 mT. The image was taken with a 12 bit CCD camera [15].

3. NONDESTRUCTIVE CHARACTERIZATION OF HTSC THIN FILMS

Local defects in the μm -range, like cracks, microscratches, structural irregularities and small holes in the HTSC layer can strongly influence the performance of HTSC thin film devices. Due to the growing number of applications—like microwave stripline filters used in telecommunication electronics—there is an increasing need for reliable characterization methods of HTSC thin films to guarantee a steady quality of devices. In practice normal light-microscopic examinations do not in any case allow to distinguish between surface impurities and real defects of the superconducting properties. Moreover HTSC thin films coated with additional gold contact layers, as often used for microwave applications, cannot be characterized. As the local critical current density is reflected in the magnetic screening behavior of high- T_c superconductors, the magneto-optical method with its lateral resolution in the μm -range has a high potential for the quality control of HTSC thin films.

In the past most magneto-optical investigations have been carried out only on small samples ($1 \times 1 \text{ cm}^2$ and smaller, see [6] and references therein), and the experimental setups that were used for these experiments are not suitable to characterize larger HTSC thin films. In particular this applies to HTSC wafers with 3" diameter, a standard size for the production of various devices. For a standard characterization of HTSC thin films a simple and fast determination of the film proper-

ties by cooling with liquid nitrogen to 77 K is desirable. However at such high temperatures the contrast in magneto-optically observed flux distributions decreases very strongly [13] because of the lower critical current density as compared to temperatures far below the critical temperature T_c (92 K in the case of YBCO). That is the reason why in contrast to the thicker YBCO crystals most magneto-optical investigations on YBCO thin films have been carried out at temperatures below 65 K.

By optimizing magneto-optics with regard to larger samples and higher magnetic sensitivity this promising method could be more widely accepted for the characterization of large HTSC thin films. In the following we will present our efforts towards this direction.

3.1. Magneto-Optical Characterization of 3" YBCO-Wafers

The investigated 3" YBCO thin film was deposited by pulsed-laser deposition [14] on both sides of an r -plane sapphire wafer with CeO_2 buffer layer. Both layers had a thickness of 300 nm. The first side had a critical current density $j_c(77 \text{ K}) = 5 \times 10^6 \text{ A/cm}^2$ and the second $j_c(77 \text{ K}) = 3.5 \times 10^6 \text{ A/cm}^2$. Both wafer sides were additionally gold coated. As a magneto-optical layer placed onto the superconductor we used a doped ferrimagnetic iron-garnet layer with in-plane magnetization grown onto 3" gadolinium-gallium-garnet substrate by liquid phase epitaxy. Further experimental details are described in [15].

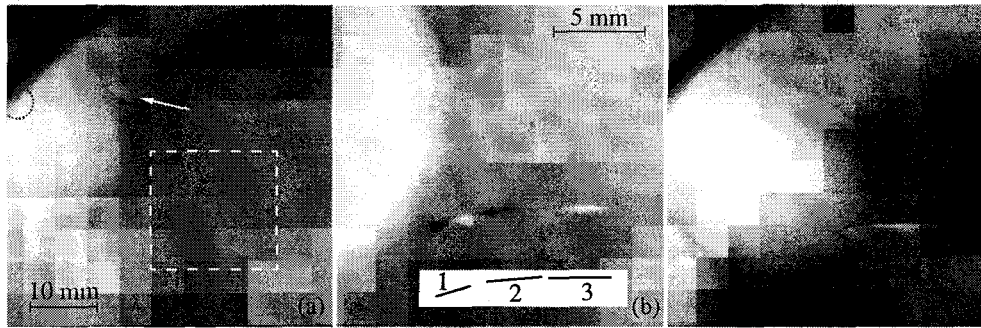


Fig. 3. Magnetic flux distribution near the edge of a 3" double-sided YBCO-Wafer at 77 K (ZFC) in different applied magnetic fields B_{ext} perpendicular to the film. The images were taken with a 16 bit CCD camera. (a) $B_{\text{ext}} = 5.0$ mT. At the position of the black dotted semicircle the substrate was held during film deposition. (b) Marked area in (a) with higher magnification and with higher external field $B_{\text{ext}} = 6.6$ mT. The influence of three defects (for dimensions see inset) on the Meissner current density leads to a characteristic black-and-white structure in the flux distribution. (c) Same magnification as in (a) upon further increase of the external field ($B_{\text{ext}} = 7.4$ mT) [15].

Figure 2 shows a full-length image of the flux distribution of a 3" double-sided YBCO-wafer. The sample was zero field cooled to a temperature of 10 K and exposed to a homogeneous magnetic field of 86 mT. During the YBCO deposition the wafer had been fixed on four positions at the edge (black arrows). At these positions, the sapphire substrate was not coated on semicircles with radius of 2 mm (see dotted semicircle in Fig. 3a). Because the screening currents have to follow more or less the perimeter of the sample, this deviation from the perfectly round disk geometry leads to a different screening current distribution and an easier flux penetration near the uncoated parts of the wafer (see below).

The effect of the sample geometry can clearly be seen in Fig. 2. Besides a more or less uniform flux penetration that points to a quite homogeneous critical current density of the wafer, one observes a more pronounced flux penetration from the uncoated parts which leads to a fourfold symmetry. This interpretation is in accordance with the homogeneous critical current density distribution of this thin film, that could be determined by inductive measurements with a lateral resolution of a few millimeters (limited by the size of a small coil used for the experiment). In contrast to the inductive method the magneto-optic technique has a much higher lateral resolution in the μm -range.

Figure 3 shows the magnetic flux distribution near the edge of the YBCO-wafer with higher magnification and lateral resolution. Compared to Fig. 2 the wafer was turned, i.e., the second side is now facing the magneto-optic indicator layer. The main difference between Fig. 2 and Fig. 3 is however that the latter shows the flux distribution at 77 K and not at 10 K. At 77 K the flux penetrates the YBCO thin film at considerable lower external field, and the contrast in the magnetic flux distribution and hence the light intensity is much weaker. To achieve an equivalent image quality we

used a CCD camera with a very high dynamic range (16 bit). Looking at the flux distribution at the lowest magnetic field in Fig. 3a) in more detail one clearly observes the influence of the uncoated semicircle, where the wafer was held during film deposition. At small magnetic fields in the Meissner state the screening currents have to flow around this uncoated part. This changed direction of the screening current shields the external field less effectively at the apex of the uncoated semicircle, and the current density has to adjust locally to higher values to screen the superconductor perfectly. With further increase of the external magnetic field flux starts penetrating the layer at this apex, because the current density exceeds the critical value j_c there first. At higher fields like in Fig. 2 on both sides of this enhanced flux penetration one clearly observes a dark line. At these so-called discontinuity lines the critical current density has a very small curvature radius and screens the external field very effectively [5, 16]. A similar influence on the flux distribu-

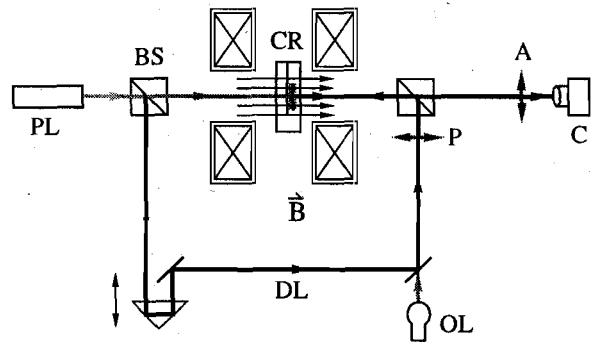


Fig. 4. Pump-probe setup used to obtain high time resolution. CR = cryostat with superconducting sample and indicator film, PL = pulse laser, BS = beam splitter, DL = delay line, OL = optional continuous light source, P = polarizer, A = analyzer, C = CCD camera.

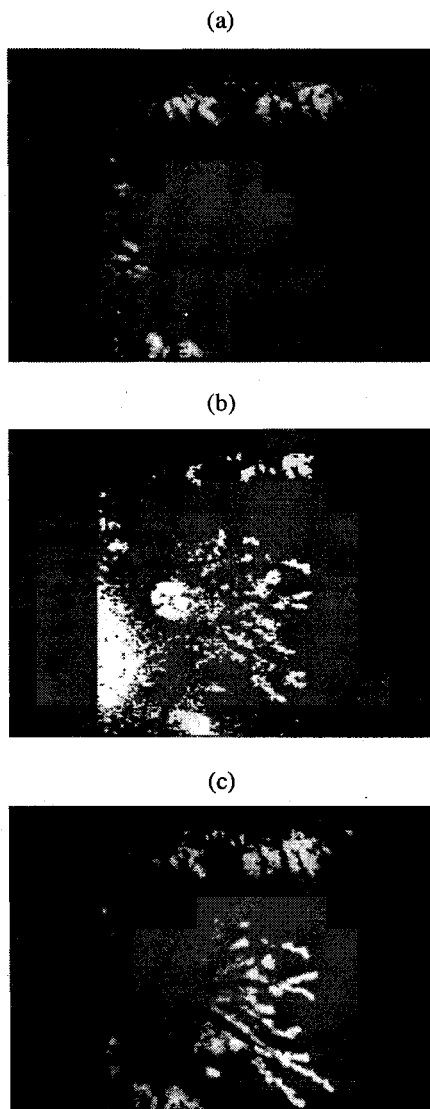


Fig. 5. Time evolution of the instability in the magnetic field distribution [1]. The frames correspond to a $4 \times 4 \text{ mm}^2$ section of the superconductor, which had been zero field cooled to $T = 1.8 \text{ K}$ before applying a magnetic field of $B_{\text{ext}} = 25 \text{ mT}$. (a) Before the laser pulse, (b) 56 ns after the laser pulse, and (c) final flux distribution. The width of the branches is $\approx 0.1 \text{ mm}$.

tion can be observed when the flux front reaches small defects in the inner part of the wafer like in Fig. 3a (white arrow).

So far we have only discussed defects which are reached by the flux front and are at least partly connected to the Shubnikov region. A different situation arises for defects which are still in the Meissner region. In contrast to a longitudinal geometry where demagnetization effects can be neglected, the Meissner state of a thin superconducting disk in a perpendicular mag-

netic field is accompanied by Meissner surface currents flowing along the *entire width* of the specimen [7]. In a flawless Meissner region of a thin film, there are no perpendicular, but only tangential magnetic field components and the magneto-optical image stays dark. In the presence of local defects the Meissner screening currents have to flow around these defects. At the resultant flux distribution the flux lines are turned towards the defect, so the normal component is decreased at the side facing the edge of the wafer and increased at the opposite side, resulting in a characteristic black-and-white structure [15, 17], which can be observed at three small cracks in Fig. 3b. The image shows the marked area in Fig. 3a with a higher magnification and a higher external field $B_{\text{ext}} = 6.6 \text{ mT}$. The exact geometry of the defects, shown in the inset of Fig. 3b, was determined magneto-optically at lower fields, where also the defects 2 and 3 separately showed the characteristic black-and-white structure (after enhancing the brightness by image processing). At higher magnetic fields like in Fig. 3b the stray fields of both defects influence each other resulting in a neutralized region between them. Under a normal light microscope these defects could not be observed, because they are covered by the gold layer.

After increasing the external magnetic field further ($B_{\text{ext}} = 7.4 \text{ mT}$) the flux front reaches the defects, the characteristic black-and-white structure disappears and again the perimeter of the defects results in an enhanced flux penetration from the defect region (Fig. 3c).

4. MAGNETIC INSTABILITY TRIGGERED BY LASER PULSE

4.1. Flux Avalanche into the Meissner State

In earlier experiments we studied the magnetic flux pattern triggered by a magnetic instability into the Meissner state of a superconducting film. These flux structures are not only of fundamental interest, but are also important from the application point of view, because they even form spontaneously and then can lead to a local destruction of the superconducting film. Figure 5 shows a sequence of magneto-optic images obtained using the pump-probe technique. One can clearly see that the dendritic structure is almost but not yet fully developed 56 ns (Fig. 5b) after triggering the instability by local heating with a focused laser pulse. For further details of the experiment the reader is referred to [1]. The most important finding is the extremely high spreading velocity of the branches. They penetrate into the superconductor at $(5 \pm 2) \times 10^4 \text{ m/s}$ which is an order of magnitude higher than the velocity of sound. In the initial stage the redistribution of flux occurs even faster at a speed that can only be estimated to $> 2 \times 10^5 \text{ m/s}$, the time resolution being limited by the pulse duration of the laser used. Therefore thermal diffusion can be excluded as a primary explanation for the phenomenon. A possible theoretical explanation of the

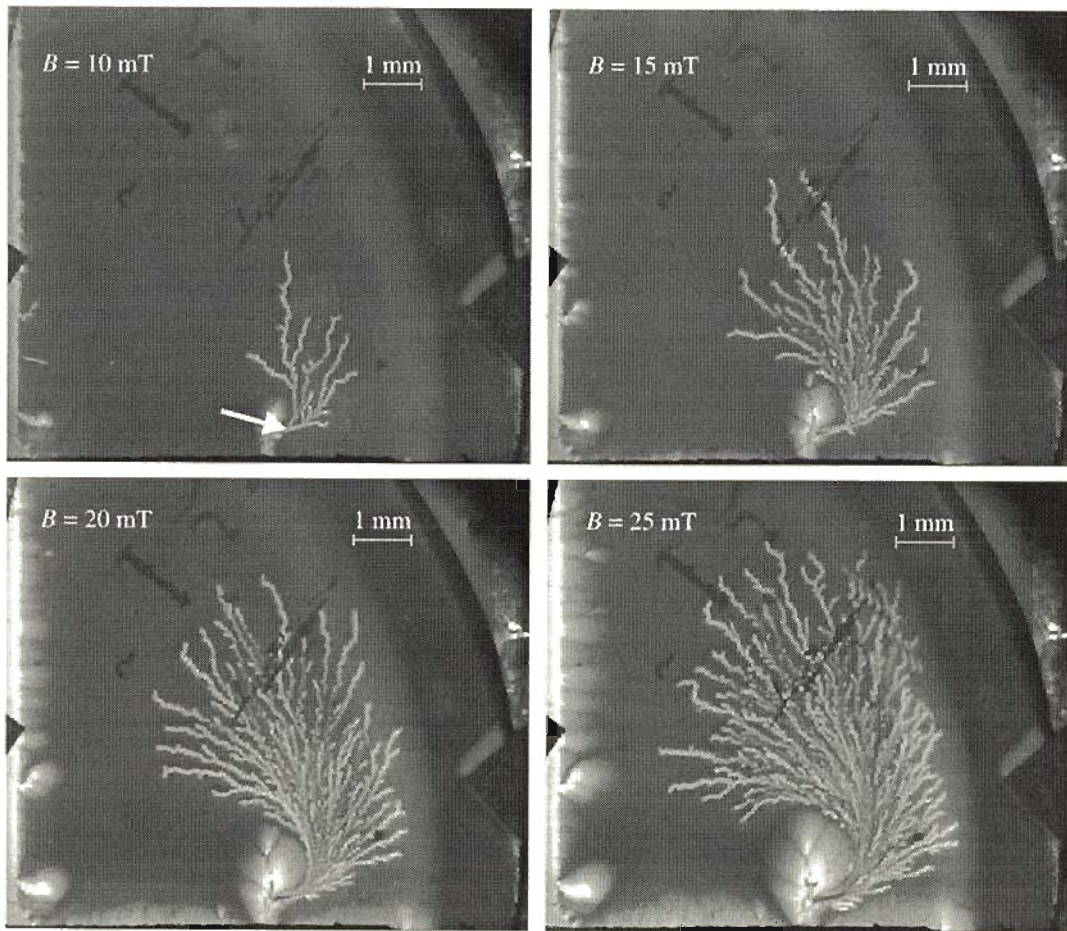


Fig. 6. Magneto-optical images of a YBCO film zero field cooled down to 10 K. The flux distribution after a 10 mJ/cm^2 laser pulse focused to a $30 \mu\text{m}$ spot close to the bottom edge of the image (arrow). Above a threshold of $B_{\text{ext}} = 7.5 \text{ mT}$ the area of the pattern increases linearly with the strength of the external magnetic field applied before the laser pulse.

phenomenon in terms of thermomagnetic shock waves has been proposed in [18].

4.2. Flux Avalanche with Varying Parameters

In order to learn more about the driving forces for the growth of the dendritic structures we extended our investigation to study the formation of the flux pattern under varying parameters like the strength of the external magnetic field, the duration of the trigger pulse and the presence of flux lines in the area before applying the trigger pulse.

For this purpose we have used epitaxial c -axis oriented $\text{YBa}_2\text{Cu}_3\text{O}_{7-\delta}$ films deposited by pulsed-laser deposition on MgO with CeO_2 buffer layer [19]. The films had a thickness of 300 nm and a critical current density of $j_c(77 \text{ K}) = 1.3 \times 10^6 \text{ A/cm}^2$.

The YBCO film was zero field cooled down to 10 K. After reaching a stable temperature an external mag-

netic field B_{ext} perpendicular to the sample surface was applied. Magnetic flux penetrated into the superconducting film first from the edges and from defects which were in contact with the edges until a local equilibrium of the flux distribution due to the pinning force and the magnetic force was reached. This induces a current distribution in the superconducting film.

In order to disturb the equilibrium of this current distribution and to initiate a magnetic instability, a pulse of a frequency doubled Nd : YAG laser ($\lambda = 532 \text{ nm}$, half width $\tau = 7 \text{ ns}$) was focused onto the film from the substrate side. The energy density in the laser spot (diameter $30 \mu\text{m}$) was up to 30 mJ/cm^2 . The sample temperature in the focus could not be measured directly, but we estimate that the temperature is well above the critical temperature.

If the perturbation is sufficiently strong, e.g., for energy densities of the laser pulse above 7 mJ/cm^2 , this triggers a magnetic instability, in which a magnetic flux avalanche penetrates into the film. Figure 6 shows a

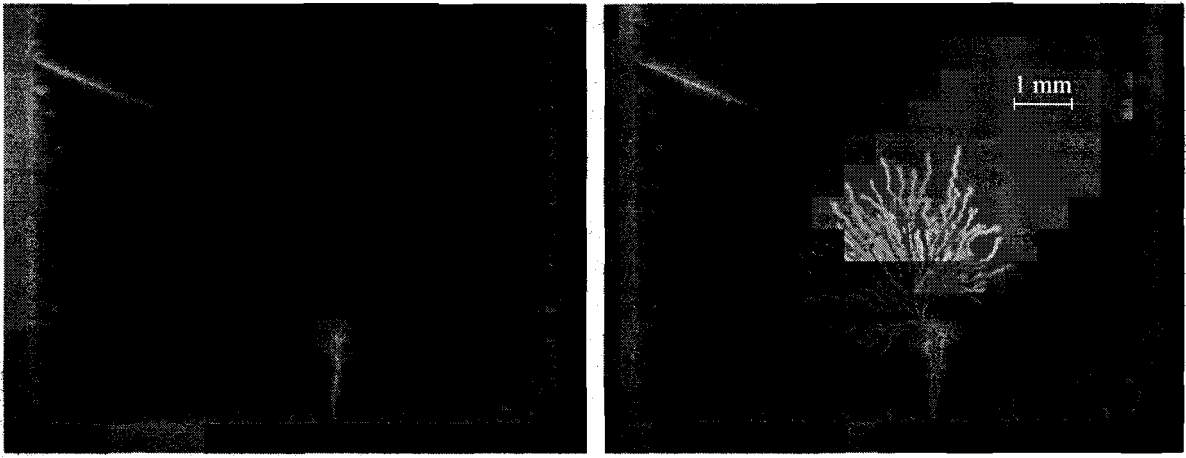


Fig. 7. Magneto-optic images before and after triggering a magnetic instability by an ultrashort laser pulse (half width $\tau = 150$ fs, energy density ≈ 10 mJ/cm², $\lambda = 819$ nm). The sample was zero field cooled to 10 K before applying a field of $B_{\text{ext}} = 19.2$ mT.

magneto-optical image of the resulting flux distribution after the laser pulse. Bright regions correspond to high magnetic flux density. In contrast to the more or less homogeneous flux fronts which propagate towards the sample center when the external field is gradually increased, this instability develops in the form of a dendritic pattern, like in Fig. 5. The total area covered by the flux branches is found to increase linearly with the external magnetic field B_{ext} above a threshold of $B_{\text{ext}} = 7.5$ mT, whereas the width of the branches (0.1 mm) remains constant within our accuracy.

To test whether flux already present in the sample influences the avalanche-like penetration we performed a series of experiments where the sample was not cooled in zero field but in an external magnetic field of well defined strength. Then the external field was increased and subsequently a trigger pulse directed onto the sample. The main result of these experiments is that the extent of the structures formed depends primarily on the change in the magnetic flux density ΔB_{ext} and is independent of the absolute values.

Another interesting question is whether the trigger pulse is of thermal nature or whether it also depends, e.g., on the strength of the electric field during the laser pulse. In order to investigate this we studied the dependence of the process on the duration of the laser pulse depositing the energy into the HTSC film. For generation of ultrashort pulses a Ti : sapphire laser was used giving half widths down to $\tau = 150$ fs. Figure 7 shows magneto-optic images taken shortly before and after such a trigger event. The structures obtained show no significant difference compared to the ones in Fig. 6 although the pulse durations differ by more than five orders of magnitude. This result strengthens the assumption that the trigger process is mainly thermal.

CONCLUSION

Concerning the magneto-optic characterization of HTSC thin films, we have demonstrated a magneto-optical apparatus which is suitable to investigate large 3" double-sided YBCO thin films. The magnetic resolution was optimized that even small defects in the Shubnikov and Meissner region could be detected at 77 K, where contrasts in the critical current are weaker and the magneto-optical characterization of HTSC thin films is much more difficult than at lower temperatures. So the apparatus can be used even under conditions where cooling with liquid helium or closed-cycle refrigerators is not available. Further we have studied magnetic instabilities induced by a laser pulse in superconducting YBCO films exposed to an external perpendicular magnetic field. The resulting flux distribution has a dendritic structure with a different flux density and their total area depends linearly on the change ΔB_{ext} above a certain threshold. The trigger process is probably purely thermal as no dependence was observed on the pulse duration over five orders of magnitude.

ACKNOWLEDGMENTS

The authors would like to thank H. Kinder, P. Berberich, W. Prusseit, R. Semerad, M. Lorenz, and H. Hochmuth for providing YBCO thin films, H. Dötsch, M. Wallenhorst, and E. Il'yashenko for providing garnet layers, and Ch. Neumann, T. Kässer, and M. Klauda for sample preparation and useful discussions. This work was supported in part by the BMBF under Grant No. FKZ 13 N 6834, the Robert Bosch GmbH, and the Konstanz Center for Modern Optics (OZK).

REFERENCES

1. Leiderer, P., Boneberg, J., Brüll, P., Bujok, V., and Herminghaus, S., 1993, *Phys. Rev. Lett.*, **71**, 2646.
2. Mints, R.G. and Rakhmanov, A.L., 1981, *Rev. Mod. Phys.*, **53**, 551.
3. Huebener, R.P., 1979, *Magnetic Flux Structures in Superconductors* (Berlin: Springer-Verlag).
4. Brüll, P., Kirchgässner, D., and Leiderer, P., 1991, *Physica C*, **182**, 339.
5. Schuster, Th., Indenbom, M.V., Koblischka, M.R., *et al.*, 1994, *Phys. Rev. B*, **49**, 3443.
6. Koblischka, M.R., 1996, *Supercond. Sci. Technol.*, **9**, 271.
7. Mikheenko, P.N. and Kuzovlev, Yu.E., 1993, *Physica C*, **204**, 229.
8. Brandt, E.H., Indenbom, M., and Forkl, A., 1993, *Europhys. Lett.*, **22**, 735.
9. Zeldov, E., Clem, J.R., McElfresh, M., and Darwin, M., 1994, *Phys. Rev. B*, **49**, 9802.
10. Huebener, R.P., Rowe, V.A., and Kampwirth, R.T., 1970, *J. App. Phys.*, **41**, 2963.
11. Dorosinskii, L.A., Indenbom, M.V., Nikitenko, V.I., *et al.*, 1992, *Physica C*, **203**, 149.
12. Wallenhorst, M., 1998, *Herstellung und Charakterisierung magnetooptischer Eisengranatfilme für nichtreziproke Wellenleiter und magnetooptische Sensoren*, PhD thesis, Universität Osnabrück.
13. Indenbom, M.V., Forkl, A., Ludescher, B., *et al.*, 1994, *Physica C*, **226**, 325.
14. Lorenz, M., Hochmuth, H., Natusch, D., *et al.*, 1996, *Appl. Phys. Lett.*, **68**, 3332.
15. Eisenmenger, J., 1999, *Reversible Laserstrukturierung und magnetooptische Charakterisierung von Hochtemperatursupraleiter-Dünnschichten*, PhD thesis, Universität Konstanz.
16. Campbell, A.M. and Evetts, J.E., 1972, *Critical Currents in Superconductors* (London: Taylor & Francis).
17. Baziljevich, M., Johansen, T.H., Bratsberg, H., *et al.*, 1996, *Appl. Phys. Lett.*, **69**, 3590.
18. Maksimov, I.L., 1994, *Physica C*, **235-240**, 3017-3018.
19. Berberich, P., Assmann, W., Prusseit, W., *et al.*, 1993, *J. of Alloys & Compounds*, **195**, 271.